12

Improving the ion thruster diagram I. Dependence of efficiency parameters on the value of magnetic field induction

© N.K. Fedyanin, M.Yu. Selivanov, D.A. Kravchenko, A.V. Sabitova

State Scientific Center of the Russian Federation „Keldysh Research Center“,
125438 Moscow, Russia
e-mail: nikita.fedyanin@gmail.com

Received March 7, 2024
Revised July 2, 2024
Accepted July 17, 2024

The current article describes the results of studies of the dependence of the efficiency parameters of an ion thruster on the magnitude of the magnetic field induction in a discharge chamber with ionization of the propellant in a direct current discharge. As part of the work, fire tests were carried out on an ion thruster with various configurations of the magnetic system, differing in the magnitude of the magnetic field induction, but having a single topology. Based on the test results, efficiency curves and radial distributions of the ion beam current density for the studied configurations were obtained. Based on the data obtained, the dependences of the efficiency parameters of the ion thruster on the magnitude of the magnetic field induction were formulated. An increase in the induction value in the discharge chamber corresponded to an increase in the discharge voltage, as well as a decrease in the uniformity of the distribution of the ion beam current density and the ion cost. The results of the work are fully consistent with earlier studies.

Keywords: electric propulsion, discharge chamber, ion optics, ion beam, ion cost, mass utilization efficiency.

DOI: 10.61011/TP.2024.11.59755.80-24

Introduction

Ion thrusters (IT) are among the most common types of electric propulsions, which have characteristic high values of specific impulse and lifespan. The main components of the IT are a discharge chamber (DC), responsible for the formation of plasma by shock ionization of the neutral component of the propellant by electrons, an ion optics (IO) that extracts ions from the plasma of the DC and creates thrust through their electrostatic acceleration, and a neutralizer that emits electrons into a beam of accelerated ions, compensating for its positive charge.

Since ITs have been developed and used as part of spacecraft since the second half of the twentieth century [1], at the moment there are many variants of circuits for each of the thruster components. IT IO differ from each other mainly in the number, material and geometry of the grids. As a rule, IO used in thrusters consist of two or three grids made of titanium, molybdenum or carbon and perforated with round apertures [2]. In most cases, the neutralizer is a hollow cathode, however, there are ITs that use high-frequency and microwave cathodes [3] to compensate for the positive charge of the ion beam. Nevertheless, ITs are classified mainly according to the type of DC. DCs with ionization of the propellant in high-frequency and microwave discharges, as well as in a direct current discharge are the most common [4].

In general, the following three main parameters are used to evaluate the efficiency of the IT DC: ion cost, mass utilization efficiency and homogeneity of the ion beam current density distribution.

The ion cost determines the energy cost of creating one ion that leaves the DC and creates thrust. This parameter directly affects the temperature of the thruster during its operation, since heating is mainly attributable to the discharge power. The discharge power decreases when the ion cost decreases, and, accordingly, the total power of the ion decreases. Thus, the lower the ion cost, the higher the efficiency of the thruster. At the same time, however, it should be noted that the effect of the ion cost on the overall efficiency becomes less significant with an increase of the specific impulse of the thruster.

Unlike ions, the neutral component of the propellant is not accelerated by the IO and leaves the thruster at thermal speeds, without making a significant contribution to the thrust. The mass utilization efficiency shows which part of the flow rate of the propellant leaves the DC without ionizing. The lower the mass utilization efficiency, the greater the consumption required by the thruster to achieve the required thrust. In addition, the IO lifespan decreases with a decrease of mass utilization efficiency, and, consequently, the IT lifespan decreases as a whole. The mass utilization efficiency is calculated as the ratio of the mass flow of ions drawn into the beam to the mass flow rate of the propellant entering the DC in a unit of time. When evaluating the effectiveness of an IT, its ion cost and mass utilization efficiency are usually considered not separately, but in combination, since they are interrelated parameters.

The homogeneity of the ion beam current density distribution is a parameter that affects the range of regulation of the ion beam current, and, accordingly, the thruster thrust. Each IO is capable of focusing a limited range of current

densities. Both the highest and lowest current densities of ions extracted from the DC should fall into this density range. Thus, the higher the homogeneity, the greater the thrust range can be provided with constant parameters of the IO. The homogeneity affects the lifespan of the IO like the mass utilization efficiency, since the grids also have the highest erosion rate in areas where the highest ion current density is extracted from the DC.

It is necessary to take into account the discharge voltage and the proportion of double-charged ions in addition to the main parameters for evaluating the efficiency of the DC. The discharge voltage determines the energy with which the ions collide with the DC surfaces located under the cathode potential, and, consequently, the rate of erosion of these surfaces. The proportion of double-charged ions shows the percentage of these particles in the ion beam. Significantly higher energy costs are required for creating a double-charged ion than for creating a single-charge ion, and double-charged ions are accelerated to high speeds in IO. The formation of double-charged ions in the DC is undesirable because they increase the value of the power required for the thruster to achieve the required thrust.

This study is devoted to DC with ionization of the propellant in a DC discharge. An idealized 0-dimensional numerical DC model of this type shows an ion cost value of less than 90 W/A at a mass utilization efficiency of 90% [4]. Since the ion cost for most of the currently developed ITs exceeds 200 W/A, it is obvious that the task of increasing the efficiency parameters of the ITs is still relevant. The main reason for the relatively low efficiency of the developed IT DC is the high surface losses of charged particles, in comparison with the simulation results. The magnitude of surface losses is attributable to the complexity of development of a sufficiently effective magnetic system (MS) which is an element that increases the residence time of charged particles in the plasma volume by reducing their mobility in the direction of part of the DC surfaces [5]. The effect of MS on the homogeneity of the ion beam current density distribution was not considered in the above-described 0-dimensional model. In fact, it is necessary to take into account the impact of MS on all efficiency parameters when creating a IT DC, which complicates the development process because of additional requirements for MS.

DC MS can be made on the basis of electromagnets or permanent magnets. Only MS based on permanent magnets are considered in this paper, since higher efficiency parameters are were achieved when they were used [6]. Generally, the DC comprises the cathode, anode and collector in addition to MS as shown in Fig. 1, *a* through which the main part of the propellant flow enters the DC.

The propellant is ionized in the DC both by primary electrons emitted by the cathode and by secondary electrons formed in the volume of the DC during the process of ionization and inelastic collisions of primary electrons [4,5,7,8]. The energy of the secondary electrons obeys the Maxwellian distribution, and averages about 5 eV [5,9–11]. Primary electrons have an energy of about 20 eV [9]. Primary electrons gain most of this energy by accelerating in the cathode potential drop $\Delta\varphi_2$, shown in Fig. 1, *b* [4,12]. It is the primary electrons that play a key role in the ionization process since the energy of primary electrons is several times higher than the energy of secondary electrons [4,5,8].

The energy the primary electrons receive is usually insufficient to reach any surface of the DC located under the cathode potential because of the presence of a potential drop $\Delta\varphi_1$ inside the hollow cathode which is not involved in the acceleration of primary electrons [4]. Since the IO screen grid is under the cathode potential, and the anode is shielded by a magnetic field, most of the primary electrons cannot reach the surfaces surrounding the plasma, and remain in its volume until the moment of ionization [7].

At least the amount of electrons necessary to maintain the discharge in the DC shall be absorbed by the anode, despite its shielding by a magnetic field. The energy of the absorbed electrons is thus removed from the volume of the DC and spent on heating the thruster structure. For this reason the discharge current shall be maintained mainly by secondary electrons with lower energy for ensuring the lowest ion cost achieving which requires consideration of two main areas of surface electron losses during the development of the DC [4,13].

The first region comprises MS poles, where the absorption of both primary and secondary electrons is present in the general case [4,5,10]. In this case, the poles are the areas in which the magnitude of the magnetic field induction has the greatest values, and the lines of tension converge and cross the outer surface of the DC [4,13]. Moving parallel to the lines of magnetic field strength, electrons can reach the surface of the DC and, in particular, the anode. One of two additional retention methods is usually used to reduce the surface loss of electrons in the pole region [4,13]. The first method is electrostatic retention: the poles are isolated from the anode and placed under the cathode potential. The second method is based on the effect of a magnetic mirror: if the increase in magnetic field induction in the pole area is large enough, then, the component of the electron velocity vector parallel to the magnetic field lines will turn to zero approaching the pole, and then will begin to grow in the direction of the decrease of the induction.

The second region is the zone between the MS poles, in which the magnitude of the induction modulus weakens moving away from them [4,13]. The lines of magnetic field strength in this area are oriented mainly parallel to the housing of the DC. In this regard, the surface losses of electrons are caused by their movement across the lines of magnetic field strength, and the theories of classical and anomalous diffusion are used to describe the losses. The largest value of the magnetic field induction modulus, the contour of which does not intersect the surface of the anode, is called closed-loop induction [7,14]. Early studies show that the value of closed-loop induction should be 50 G foe the most effective retention of electrons between the poles of the MS and ensure the lowest ion cost [7,15]. In

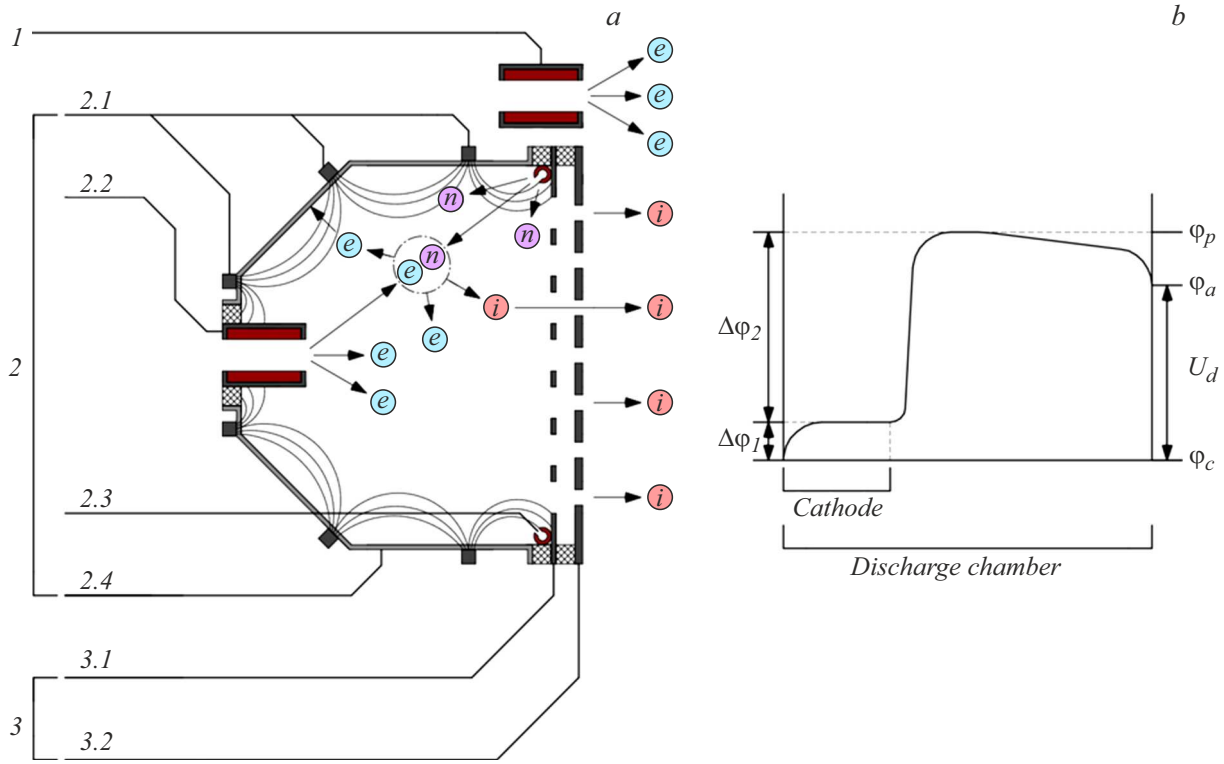

Figure 1. *a* — IT diagram: *1* —neutralizer; *2* — GRK; *2.1* — MS; *2.2* —cathode; *2.3* — anode; *2.4* —collector; *3* – IO; *3.1* —screen grid; *3.2* — accelerator grid; *b* — distribution of potential in DC: U_d —discharge voltage; φ_c —cathode potential; φ_a —anode potential; φ_p —plasma potential; $\Delta\varphi_1$ — potential drop inside the hollow cathode; $\Delta\varphi_2$ — cathode potential drop [4].

the framework of later studies, it is recommended to use the largest possible closed-loop induction for the same purposes, in which the number of electrons necessary to maintain the discharge in the DC is absorbed by the anode [7,16]. In the general case, only the losses of secondary electrons are considered in the zone between the MS poles, since the losses of primary electrons in it are insignificant in comparison with their losses in the field of poles [4,5,7,17–19].

The surface recombination of these particles has a key impact on the ion cost because the formation of plasma for the subsequent extraction of ions from it using IO the main task of the DC [5]. The ion cost can be decreased by reducing the proportion of ions recombining on DC surfaces and increasing the proportion of ions extracted by IO [6]. The cathode, the screen grid and the magnetic field-shielded surfaces, which, in particular, include the anode are the main areas of ion recombination [4,5].

One of the simplest and most effective methods of reducing the ion cost is to increase the effective transparency of the IO for ions which is a parameter showing which part of the ion current from the DC to the screen grid is extracted and forms an ion beam, and which is recombined on the grid surface [4,14]. The simulation results show a 20% decrease of the ion cost in the IT DC with an increase of the effective transparency of its IO for ions from 70 to 80% [14]. Also, the transparency of the IO for the neutral component of the propellant is an equally important parameter that shows which part of the flow of the non-ionized propellant to the screen grid leaves the DC [4]. The reduction of this parameter makes it possible to increase mass utilization efficiency with constant discharge parameters.

In contrast to the ion cost, the homogeneity of the ion beam current density distribution is usually negatively affected by the limitation of the mobility of charged particles by the magnetic field in the DC. The current density of the ion beam in the center of the IO for IT with DC with ionization of the propellant in a DC discharge can be several times higher than at the periphery, therefore the homogeneity is usually considered only in the radial direction. The experimental results show that the homogeneity of the plasma near the IO which depends mainly on the magnetic field has the key impact on the homogeneity of the ion beam current density distribution [5,14,20]. The ITs near the IO of which the magnitude of the magnetic field induction modulus is less than 10 G have the most homogeneous ion beam current density distributions [21–23]. Other areas of the magnetic field also have an impact in addition to the area near the IO. For example, a strong magnetic field in the central region of the DC can results in the excessive retention of primary electrons on the axis of the thruster [7,10,14]. This will result in a high concentration of ions in this area, which will also negatively affect the homogeneity of the ion beam current density distribution.

The task of MS optimization has been repeatedly raised by various IT developers throughout almost the entire existence of these devices. Efforts for creation of MS for IT DC were taken in Japan, China, the UK and the Russian Federation, but the greatest results were achieved in the USA in the early two-thousands [4,24]. In addition to the above-mentioned work for the optimization of MS and DC in general, it is also possible to highlight experimental studies of the possibility of miniaturization of this node, which accompanied the development of the MiXI IT [9,25–27]. The highest efficiency to date have been demonstrated by ion thrusters XIPS-25 [4,21,28,29], NSTAR [4,5,7,9,16,30–33], NEXIS [4,14,23,34] and NEXT [22,31,35,36], developed in the USA, and ion thrusters with IO perforated area diameter of 35 cm [37–40], developed in Japan. The parameters corresponding to the most efficient operating modes of all the above-described thrusters or their modifications are listed in Table 1.

The DC circuits of all the thrusters listed in Table 1 are similar. The MS of each of them is based on permanent magnets, and the magnetic field in the DC has a homogeneous arched structure, where areas with magnetic field induction of more than 10 G are localized near the anode. The efficiency parameters of these thrusters vary significantly. At the moment, XIPS-25 [28] has the lowest ion cost, however, the available information about this thruster is not sufficient to analyze the parameters achieved by it. More obvious is the method of ion cost reduction used for the development of the NEXT IT, namely, increasing the effective transparency of the IO for ions. The effective transparency of IO IT is at the level of 70% on average, this parameter reaches 86% for IO of NEXT IT [36].

The work for the optimization of MS IT was conducted in the Russian Federation mainly by „Keldysh Research Center“. Relevant studies include a series of tests that compared with each other the MS configurations consisting of 3 and 4 annular permanent magnets as well as with MS based on electromagnets [41]. The aim of the paper was to determine the dependence of the efficiency parameters on the topology of the magnetic field, as well as to identify the topology corresponding to the highest values of these parameters. According to the results of study, MS based on permanent magnets showed a better homogeneity of the ion beam current density distribution and a higher ion cost in comparison with MS based on electromagnets. At the same time, the use of permanent magnets made it possible to achieve the required values of the mass utilization efficiency of MS at lower discharge voltages. It should be taken into account that the efficiency parameters of DC with MS based on electromagnets were obtained with the optimal value of the magnetic field induction, which was adjusted during the tests by changing the current in the winding of the electromagnets. It is obvious that the efficiency parameters of the DC with MS based on permanent magnets could be improved by a similar optimization, however, in this case it would require stopping the tests and interfering with the design of the IT. The studied configurations would have to be divided into sub-configurations, which would correspond to the same topology of the magnetic field, but different values of its induction [41]. Due to the considerable complexity of these studies, they were included in a separate series of tests described in this paper, the purpose of which is to determine the dependence of the DC efficiency parameters on the magnitude of the magnetic field induction without changing its topology.

Table 1. IT parameters

IT	c_i, W/A	η_m,%	U_d, V
XIPS-25 [28]	122	89	28.0
NSTAR [5]	168	90	25.6
NEXIS [23]	170	92	26.3
NEXT [31]	140	90	24.0
35 cm [38]	140	90	32.3

Note. c_i — ion cost, η_m — mass utilization efficiency, U_d —discharge voltage.

1. Item under test

The prototype of IT-200PM thruster shown in Fig. 2 was tested in this study. This thruster was developed on the basis of the ID-200KR and has a power of 3 kW [41].

IO of ID-200PM consists of screen and accelerator grids made of carbon-carbon material having a flat shape and a diameter of the perforated area 200 mm. The transparency of the IO of ID-200PM for neutral atoms is 17%, the calculated dependence of the effective transparency of the IO for xenon ions on their current density is shown

Figure 2. Appearance of prototype of ID-200PM.

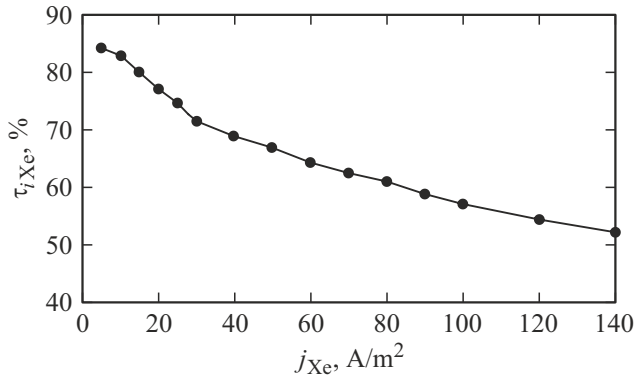

Figure 3. Dependence of the effective transparency of IO of ID-200PM for xenon ions $\tau_{i\mathrm{Xe}}$ on their current density from DC to screen grid j_{Xe}.

in Fig. 3. The DC cathode and the thrust neutralizer are hollow cathodes with emitters made of porous tungsten impregnated with barium compounds. The DC housing consisting of cylindrical and conical parts is used as an anode in the IT. The main part of the flow of the propellant is supplied to the DC through a collector located near the IO, in addition, a fixed flow value enters the chamber through the cathode.

The diameter of the housing of the DC of ID-200PM is 240 mm and exceeds the diameter of the perforated area of the IO, which is attributable both to the requirements for the design of the thruster and to an increase of the homogeneity of the current density distribution of the ion beam. The requirements for the thruster design comprise the need to place the collector and part of the MS near the IO without overlapping its perforated area. An increase of the homogeneity of the ion beam current density distribution is achieved by cutting off the current of low-density ions from the peripheral region of the plasma, where a magnetic field of more than 10 G is present [14].

The three-pole circuit, which showed the highest characteristics during the first series of experiments, was selected as the initial configuration of the MS, on the basis of which the dependence of the parameters of the DC efficiency on the magnitude of the magnetic field induction was studied [41]. The distribution of the magnetic field induction module in the ID-200PM DC corresponding to this configuration is shown in Fig. 4, *c*.

It is significant that a lower ion cost was achieved during the first series of experiments when a three-pole configurations of MS was used than in case of usage of the four-pole configuration [41]. The results of numerical simulation show that the majority of not only primary electrons, but also secondary electrons are absorbed in the region of the poles located under the anode potential [10]. Ion recombination occurs more evenly on the surfaces of the DC, but nevertheless, most of the ions, in addition to the screen grid and cathode, also recombine precisely in the region of the poles [10]. Thus, the result obtained is completely consistent with earlier study, which states that an increase of the number of poles with equal induction of a closed circuit, as a rule, leads to an increase of the ion cost [6,13,18].

The MS of the configuration selected for the start of the current operation consists of three annular permanent magnets and a ferromagnetic flange located near the IO. Sa_2Co_{17} was selected as a permanent magnet material since it is the most high-temperature rear earth magnet of the available rare earth magnetic materials, the maximum operating temperature of which is 350°C. Permanent magnets are placed close to the housing of the DC, their axis of magnetization is directed normal to it, and they are separated from the plasma volume by a sheet of 0.5 mm thick steel. The small distance between the permanent magnets and the plasma volume makes it possible to achieve the largest possible magnitude of the magnetic field induction modulus in the pole region, which exceeds 2000 G for the selected MS configuration. The pole regions are the main places of surface losses of charged particles and for this reason the magnitude of the induction modulus in pole regions has a key impact on the parameters of thruster efficiency because, since the efficiency of retention of charged particles depends on it [17].

The magnetic field in the DC has a uniform arched structure, where areas with magnetic field induction of more than 10 G are localized on the periphery of the DC, and the induction of a closed circuit is about 30 G. The ferromagnetic flange in this configuration constitutes some kind of an additional pole in the DC at the boundary with IO. Most lines of magnetic field strength close on the flange due to its high magnetic permeability, weakening the magnitude of induction near the IO. Since the magnitude of the magnetic field induction on the flange surface is orders of magnitude smaller than in the region of poles formed by permanent magnets, the effect of a magnetic mirror is not observed on it. In this case, electron retention in the plasma volume is achieved by the electrostatic method by placing the flange under the cathode potential. An analogue of this solution is used in the DC circuit of IT T6 [42], developed in the UK, as well as almost any IT with MS based on electromagnets.

Three additional MS configurations were developed for the purposes of this study, which differ from each other and from the original in the magnitude of the magnetic field induction. The induction magnitude was regulated by changing the thickness of the annular permanent magnets, i.e. the distance between their north and south poles. Changing the width of the magnets was not used, as it would entail an increase of the area of the poles, which would result in additional differences between the configurations. The distributions of the magnetic field induction module in the ID-200PM DC corresponding to the developed configurations are shown in Fig. 4, *a, b, d*.

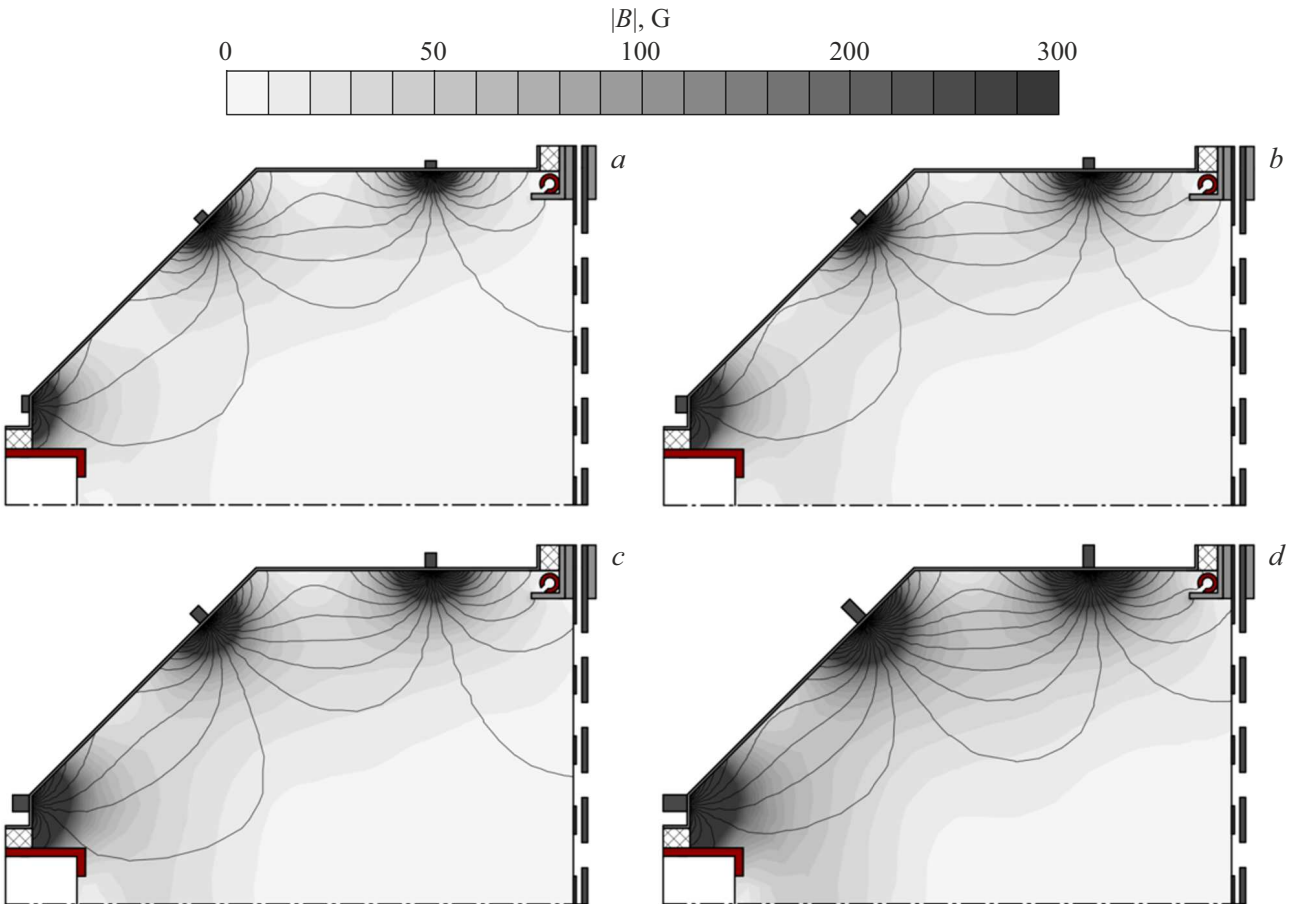

Figure 4. Distributions of the magnetic field induction modulus $|B|$ in ID-200PM DC corresponding to the studied MS configurations: *a* — configuration 1; *b* — configuration 2; *c* —configuration 3; *d* — configuration 4.

2. Experimental setup

Tests for this study were performed using the test bench of „Keldysh Research Center" KVU-90, designed for testing electric propulsions and shown in Fig. 5. The test bench has a vacuum chamber with a diameter of 3.8 m and a volume of 90 m^3, cryogenic pumps with a total xenon pumping capacity of 140 m^3/s, as well as control systems, power supply and propellant supply systems [43].

Inert gases (xenon, krypton and argon) and their mixtures can be used as a propellant for electric propulsions tested using the test bench. Two pre-chambers of test bench KVU-90 make it possible to perform operational tests and replace thrusters without inflow of the atmosphere into the main part of the vacuum chamber. The thrust measuring device ensures the measurement of thruster thrust in the range from 20 mN to 2 N. The probe diagnostics system of the test bench allows for non-contact studies of the jet parameters of thrusters [43].

The current density distribution of the ion beam was measured during the tests using a Faraday probe. The probe

Figure 5. Appearance of test bench KVU-90 [43].

was mounted on a bracket attached to a carriage, which was moved by a stepper motor. Current measurements were carried out in increments 2.25 mm. The distance from the accelerator grid to the collecting surface of the probe collector at each measurement point was 28.5 mm, collector diameter was 10 mm.

3. Test procedure

All four studied MS configurations were tested with identical DC and IT designs by replacing one set of permanent magnets with another. An IT control system with two stabilization circuits was used during testing: the first circuit maintained the ion beam current at 1.25 A by regulating the discharge current, the second circuit maintained the discharge voltage at a predetermined level by regulating the flow of the propellant into the collector. The potentials of the screen and accelerator grids were 2000 V and −300 V, respectively. The support current of the DC cathode was zero, the support current of the neutralizer was 1 A. Xenon was used as the propellant. The pressure in the vacuum chamber did not exceed $5.0 \cdot 10^{-3}$ Pa.

The MS configurations were compared based on the discharge voltage and three main parameters characterizing the efficiency of the IT DC: ion cost, mass utilization efficiency and homogeneity of the ion beam current density distribution.

The ion cost was calculated as the ratio of the discharge power to the ion beam current according to the formula (1). Since the proportion of double-charged ions was not measured in the experiment, the current in the screen grid circuit was used as the ion beam current in this formula.

$$c_i = \frac{I_d \cdot U_d}{I_b}, \tag{1}$$

where I_d —discharge current, [A]; U_d — discharge voltage, [V]; I_b — ion beam current, [A].

The mass utilization efficiency was calculated using the formula (2) as the ratio of the mass flow of xenon ions corresponding to the current in the screen grid circuit to the mass flow rate of the propellant entering the DC in the unit of time.

$$\eta_m = \frac{I_b \cdot M_{\mathrm{Xe}}}{\dot{m} \cdot e}, \tag{2}$$

where I_b — ion beam current, [A]; M_{Xe} — xenon atom mass, [kg]; $\dot{m}$ — total flow of the propellant in the DC, [kg/s]; e — electron charge, [C].

The homogeneity of the ion beam current density distribution was estimated using the inhomogeneity coefficient, which is equal to the ratio of the highest current density of the ion beam to the average area of the IO according to the formula (3). The highest density was calculated by averaging the current densities in the central region of the IO with the diameter of 20 mm for reducing the impact of measurement errors on the results of comparing MS configurations.

$$\eta_n = \frac{j_{\max}}{j_{avg}}, \tag{3}$$

where $j_{\max}$ — the highest ion beam current density, [A/m^2]; j_{avg} — the average ion beam current density, [A/m^2].

During the tests to determine the ion cost and mass utilization efficiency, the discharge voltage was changed in increments of 0.5V, in a range ensuring the maintenance of the mass utilization efficiency value from 75 to 95%. Additional operation modes of the IT at stabilized discharge voltage values were ensured by changing the flow rate of the propellant into the cathode in the range from 0.3 to 0.45 mg/s in increments of 0.05 mg/s.

The ion beam current density distribution was measured in the radial direction. The flow rate of the propellant into the cathode was 0.35 mg/s during measurement, and the mass utilization efficiency of about 90% was maintained by the discharge voltage. The distribution was measured by the probe with an ammeter was installed in the circuit that was connected in series to the „ground“ terminal. The ammeter readings were used as measurement results. A power source was sequentially installed in the circuit to cut off electrons from the beam plasma, ensuring the potential of the probe collector minus 30 V. The probe passed the measured region of the ion beam twice during the experiment (in the forward and reverse directions), and the results were averaged when calculating the final values.

4. Test results

The test results for determining the ion cost and mass utilization efficiency are a series of efficiency curves — dependences of the ion cost on the mass utilization efficiency of the IT DC. Fig. 6 shows the efficiency curves for the propellant flow into the cathode of 0.3, 0.35, 0.4 and 0.45 mg/s, respectively. The intervals of change of the discharge voltages, ensuring the range of mass utilization efficiency specified in the test procedure (from 75 to 95%), are listed in Table 2.

The results of measurements of the radial current density distribution of the ion beam are shown in Fig. 7, where the abscissa axis is the distance from the IT axis, and the ordinate axis is the current recorded by the probe at this distance normalized to the ion beam current of the corresponding configuration of the MS. The point „0“ on the abscissa axis corresponds to the IT axis. The value of the normalized current was introduced instead of the current density, since different ion beam currents corresponded to different configurations of the MS during measurements. The inhomogeneity coefficients corresponding to the obtained radial distributions of the ion beam current density are also listed in Table 2.

5. Discussion of findings

A noticeable decrease of the ion cost is observed when considering the efficiency curves obtained from the test results in case of switching to MS configurations with greater magnetic field induction. The ion cost decreases with an increase of the induction value with the exception of several modes of operation, in addition, this dependence persists with a change of the flow of the propellant into the cathode and collector. At the same time, the rate of decrease is not monotonous. Transition from configuration 1 to

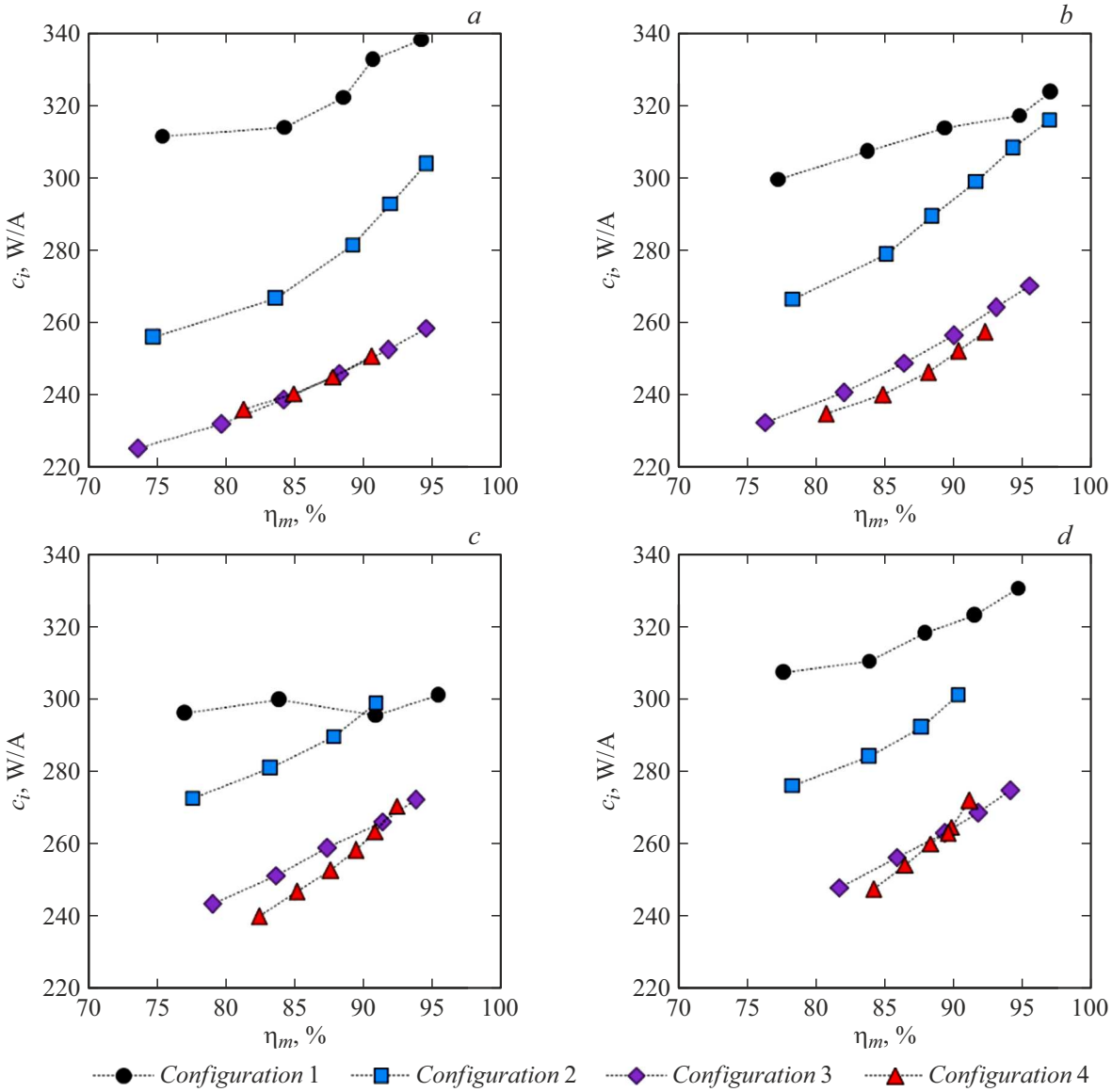

Figure 6. Dependences of the price of ion c_i on mass utilization efficiency η_m (efficiency curves) for studied MS configurations at propellant flow in cathode: *a* — 0.3; *b* — 0.35; *c* — 0.4; *d* — 0.45 mg/s.

configuration 2 and from configuration 2 to configuration 3 corresponds to a decrease of the ion cost by an average of more than 30 W/A, while the differences of the efficiency curves of configuration 3 and configuration 4 are not significant. Perhaps the result obtained is associated with the peculiarities of the increase of the induction of the magnetic field in the DC. The closed loop induction increases from 30 to 50 G in case of the transition from configuration 3 to configuration 4, but the induction modulus in the pole region almost does not change jcite13. It can be assumed that, by analogy with the Ref. [6,13] any further increase of induction is no longer advisable in the studied topology of the magnetic field with closed-loop induction of 30 G, since the surface losses of charged particles in the region between the poles become insignificant in comparison with their losses in the region of the poles. In this case, the efficiency curves of configuration 3 and configuration 4 will not have any significant differences, since they both ensure approximately equal efficiency of retention of charged particles in the area of poles.

The discharge voltage increased with the increase of the magnetic field induction. All the values of the discharge voltage obtained during the experiments are within the acceptable range, at which the erosion of cathode surfaces by single-charged ions is insignificant. Despite this, the MS configurations that ensure the lowest discharge voltages are considered optimal, since there is a proportion of double-charged ions in each DC, which have twice as much energy during the bombardment of surfaces and can cause significant erosion.

Measurements of the radial distribution of the ion beam current density showed a decrease of homogeneity with

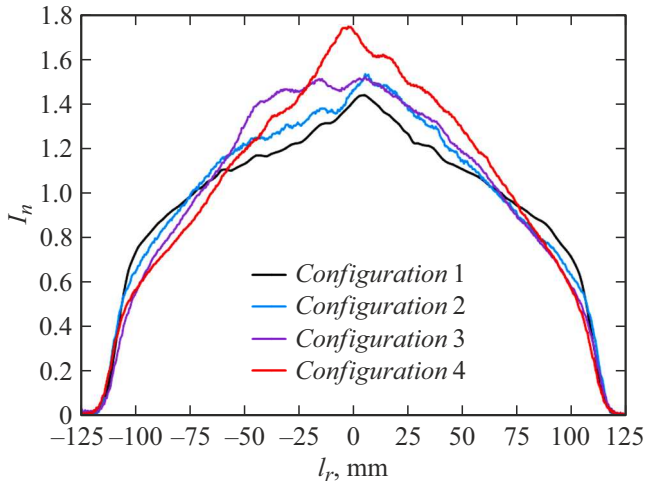

Figure 7. Dependence of the normalized current per probe I_n on distance from IT axis l_r for studied MS configurations.

Table 2. IT parameters for the studied MS configurations

Item under test	U_d, V	η_n
ID-200PM configuration 1	21.7–23.7	1.37
ID-200PM configuration 2	21.7–24.2	1.44
ID-200PM configuration 3	22.5–25.5	1.48
ID-200PM configuration 4	24.6–27.0	1.66

Note. U_d — discharge voltage, η_n — inhomogeneity coefficient.

an increase of the magnetic field induction. The result is generally consistent with earlier studies [5,14,20]. The decrease of homogeneity is attributable to the increase of induction in this study taking place throughout the entire volume of the DC, including near the IT. For example, the magnitude of the induction module near the entire perforated area of the IT is less than 10 G in configuration 1, and the contour of the induction module 10 G crosses the surface of the screen grid at a distance of about 50 mm from the IT axis in configuration 4.

A comparative analysis of the results obtained in this study with the results published earlier in the article devoted to determining the optimal topology of magnetic fields [41] shows a significant decrease of the efficiency parameters in case of usage of the latest tested MS configuration. In addition, the configuration 3 tested in both studies showed significantly lower efficiency parameters during later tests. The discrepancies in the parameters are probably caused by the use of different IO for the first and second series of tests. Also, a more advanced probe diagnostics system was used in the current study, which could affect the measurement results. Similar conclusions can be applied to the comparison of the results of the current study with the results of the IT tests provided in Table 1. The effective transparency of IO of ID-200PM during the measurement of efficiency curves was about 63%. It can be argued based on the dependence given in the Ref. [14] that when a number of tested MS configurations will show an ion cost of less than 180 W/A with a mass utilization efficiency of 90% in case of increase of the effective transparency of IO of ID-200PM to the level of IO of IT NEXT (86%), . Thus, the efficiency parameters of tested MS configurations are similar to those listed in Table. 1, and the results of the comparative analysis are primarily associated with the disadvantages of the IO used.

A more detailed study of the dependence of the IT efficiency parameters on the characteristics of the magnetic field is one of the priority goals of further research based on the results of the work. The MS configurations studied in this paper do not allow for an optimization of parameters independently of each other. For example, the lowest ion costs were obtained during the tests of configuration 3 and configuration 4, which corresponded to the highest values of magnetic field induction in DC. A completely opposite result was obtained during measurements of the ion beam current density distribution, where the lowest inhomogeneity coefficient has a configuration of 1, which corresponds to the lowest induction value.

Obviously, the optimization of one parameter has a negative effect on the other for tested MS configurations. The reason for this, as already mentioned, is that an increase of induction in the current work during the transition from one MS configuration to another occurs throughout the entire volume of the DC, including near the IO. In this case, DC with MS ensuring a magnetic field induction modulus of less than 10 G near the IT regardless of the magnitude of the closed-loop induction is of interest for subsequent studies.

Conclusion

This paper describes the results of studies of the dependence of IT efficiency parameters on the magnitude of magnetic field induction in a DC with ionization of the propellant in a DC discharge. Fire tests of various MS configurations of the IT DC constitute the main part of the study. The experimental prototype of ID-200PM thruster is the item under test in this study. The studied MS configurations consist of three annular permanent magnets and a ferromagnetic flange located near the IT. Sa_2Co_{17} is selected as the material of permanent magnets. The magnetic field in the DC has a uniform arched structure, where regions with magnetic field induction of more than 10 G are localized near the anode. The MS configurations differ from each other in the magnitude of the magnetic field induction, but at the same time they have the same topology. The induction magnitude was regulated by changing the thickness of the annular permanent magnets, i.e. the distance between their north and south poles. The MS configurations were compared based on the discharge voltage and three main parameters characterizing the efficiency of the IT DC: ion cost, mass

utilization efficiency and homogeneity of the ion beam current density distribution.

Efficiency curves and radial distributions of ion beam current density for the studied MS configurations were obtained based on the test results, and the dependences of the IT DC efficiency parameters on the magnitude of the magnetic field induction were defined. An increase of the magnitude of the magnetic field induction in the DC corresponded to an increase of the discharge voltage, as well as a decrease of the homogeneity of the ion beam current density distribution and the ion cost.

Te direction of its further improvement was defined based on the obtained data for the used magnetic field topology. This topology also significantly increases the magnetic field induction modulus near the IO , with an increase of the closed-loop induction, which results in a decrease of the homogeneity of the ion beam current density distribution. Thus, the optimization of one parameter has a negative effect on the other for tested MS configurations. In this case, DC with MS ensuring a magnetic field induction modulus of less than 10 G near the IT regardless of the magnitude of the closed-loop induction is of interest for subsequent studies.

Conflict of interest

The authors declare that they have no conflict of interest.

References

[1] R.J. Jahn. *Physics of Electric Propulsion* (Mc-Graw Hill Book Company, NY., St. Louis, San-Francisco, Toronto, London, Sydney, 1968)

[2] M. Sangregorio, K. Xie, N. Wang, N. Guo, Z. Zhang. Chinese J. Aeronautics, **31** (8), 1635 (2018). DOI: 10.1016/j.cja.2018.06.005

[3] D.R. Lev, I.G. Mikellides, D. Pedrini, D.M. Goebel, B.A. Jorns, M.S. McDonald. Rev. Modern Plasma Phys., **3** (1), Art. Num. 6 (2019). DOI: 10.1007/s41614-019-0026-0

[4] D.M. Goebel, I. Katz. *Fundamentals of Electric Propulsion* (John Wiley & Sons, Inc., 2008), DOI: 10.1002/9780470436448

[5] A. Sengupta. J. Appl. Phys., **105** (9), 093303 (2009). DOI: 10.1063/1.3106087

[6] T. Ogunjobi, J.A. Menart. *Computational Study of Ring-Cusp Magnet Configurations that Provide Maximum Electron Confinement*. 42nd AIAA/ASME/SAE/ASEE Joint Propulsion Conf. and Exhibit, 2006-4489, 2006. DOI: 10.2514/6.2006-4489

[7] R.E. Wirz, D.M. Goebel. *Ion Thruster Discharge Performance per Magnetic Field Topography*. 42nd AIAA/ASME/SAE/ASEE Joint Propulsion Conf. and Exhibit, 2006-4487, 2006. DOI: 10.2514/6.2006-4487

[8] S. Mahalingam, J.A. Menart. *Computational Model Tracking Primary Electrons, Secondary Electrons and Ions in the Discharge Chamber of an Ion Engine*. 41st AIAA/ASME/SAE/ASEE Joint Propulsion Conf. and Exhibit, 2005-4253, 2005. DOI: 10.2514/6.2005-4253

[9] R.E. Wirz. *Discharge Plasma Processes of Ring-Cusp Ion Thrusters*. Dissertation, 2005.

[10] S. Mahalingam, J.A. Menart. *Physical Parametric Studies in an Ion Engine Discharge Chamber Using a PIC-MCC Simulation*. 44th AIAA/ASME/SAE/ASEE Joint Propulsion Conf. and Exhibit, 2008-4733, 2008. DOI: 10.2514/6.2008-4733

[11] D.A. Kravchenko, A.A. Shagayda, M.Y. Selivanov, A.S. Shashkov, D.Y. Tomilin, I.A. Khmelevskoi, A.S. Lovtsov. J. Propulsion Power, **38** (12), 1 (2022). DOI: 10.2514/1.B38405

[12] B. Bias, B. Penkal, M. Jonell, J.A. Menart, S. Mahalingam. *Off Design Simulation Results of Several Operating Conditions of the NEXT Discharge Chamber*. 47th AIAA/ASME/SAE/ASEE Joint Propulsion Conf. and Exhibit, 2011-5660, 2011. DOI: 10.2514/6.2011-5660

[13] W. Bennett, T. Ogunjobi, J.A. Menart. *Computational Study of the Effects of Cathode Placement, Electron Energy, and Magnetic Field Strength on the Confinement of Electrons*. 43rd AIAA/ASME/SAE/ASEE Joint Propulsion Conf. and Exhibit, 2007-5248, 2007. DOI: 10.2514/6.2007-5248

[14] D.M. Goebel, J.E. Polk, A. Sengupta. *Discharge Chamber Performance of the NEXIS Ion Thruster*. 40th AIAA/ASME/SAE/ASEE Joint Propulsion Conf. and Exhibit, 2004-3813, 2004. DOI: 10.2514/6.2004-3813

[15] J.R. Beattie, J.N. Matossian. *Inert-gas Ion Thruster Technology*. NASA Contract Report, NAS 3-23860, 1992.

[16] A. Sengupta. *Experimental Investigation of Discharge Plasma Magnetic Confinement in the NSTAR Ion Thruster*. 41st AIAA/ASME/SAE/ASEE Joint Propulsion Conf. and Exhibit, 2005-4069, 2005. DOI: 10.2514/6.2005-4069

[17] S. Deshpande, S. Mahalingam, J.A. Menart. *Computational Study of Primary Electrons in the Cusp Region of an Ion Engine's Discharge Chamber*. 40th AIAA/ASME/SAE/ASEE Joint Propulsion Conf. and Exhibit, 2004-4109, 2004. DOI: 10.2514/6.2004-4109

[18] S. Mahalingam, J.A. Menart. J. Propulsion Power, **23** (1), 69 (2007). DOI: 10.2514/1.18366

[19] S. Mahalingam, J.A. Menart. *Primary Electron Modeling in the Discharge Chamber of an Ion Engine*. 38th AIAA/ASME/SAE/ASEE Joint Propulsion Conf. and Exhibit, 2002-4262, 2002. DOI: 10.2514/6.2002-4262

[20] R.E. Wirz, D.M. Goebel. Plasma Sources Sci. Technol., **17** (3), 035010 (2008). DOI: 10.1088/0963-0252/17/3/035010

[21] D.M. Goebel, J.E. Polk, I. Sandler, I.G. Mikellides, J.R. Brophy, W.G. Tighe, K. Chien. *Evaluation of 25-cm XIPS Thruster Life for Deep Space Mission Applications*. 36th International Electric Propulsion Conf., 2009-152, 2009.

[22] J.R. Anderson, J.S. Snyder, J.L. Van Noord, G.C. Soulas. *Thermal Development Test of the NEXT PM1 Ion Engine*. 43rd AIAA/ASME/SAE/ASEE Joint Propulsion Conf. and Exhibit, 2007-5217, 2007. DOI: 10.2514/6.2007-5217

[23] J.E. Polk, D.M. Goebel, J.S. Snyder, A.C. Schneider, L.K. Johnson, A. Sengupta. Rev. Scientif. Instrum., **83** (7), 073306 (2012). DOI: 10.1063/1.4728415

[24] A.S. Lovtsov, D.A. Kravchenko, D.A. Tomilin, A.A. Shagaida. Fizika Plazmy, **48** (9), 792 (2022) (in Russian). DOI: 10.31857/S0367292122600339

[25] B. Dankongkakul, R.E. Wirz. Plasma Sources Sci. Technol., **27** (12), 125001 (2018). DOI: 10.1088/1361-6595/aae63c

[26] S.A. Samples, R.E. Wirz. *Development Status of the Miniature Xenon Ion Thruster*. 36th International Electric Propulsion Conf., 2019-143, 2019
[27] S.A. Samples, R.E. Wirz. Plasma Research Express, **2** (2), 025008 (2020). DOI: 10.1088/2516-1067/ab906d
[28] J.R. Beattie, J.N. Matossian. R.R. Robson. J. Propulsion Power, **6** (2), 145 (1990). DOI: 10.2514/3.23236
[29] K. Chien, S.L. Hart, W.G. Tighe, M.K. De Pano, T.A. Bond, R. Spears. *Development Status of the Miniature Xenon Ion Thruster*. 29th International Electric Propulsion Conf., 2005-315, 2005
[30] J. Foster, G. Soulas, M. Patterson. *Plume and Discharge Plasma Measurements of an NSTAR-type ion thruster*. 36th AIAA/ASME/SAE/ASEE Joint Propulsion Conf. and Exhibit, 2000-3812, 2000. DOI: 10.2514/6.2000-3812
[31] D.A. Herman. *The Use of Electrostatic Probes to Characterize the Discharge Plasma Structure and Identify Discharge Cathode Erosion Mechanisms in Ring-Cusp Ion Thrusters*. Dissertation, 2005.
[32] A. Sengupta, D.M. Goebel, A. Owens. *Neutral Density Measurements in an NSTAR Ion Thruster*. 42nd AIAA/ASME/SAE/ASEE Joint Propulsion Conf. and Exhibit, 2006-4491, 2006. DOI: 10.2514/6.2006-4491
[33] R.E. Wirz, D.M. Goebel. Plasma Sources Sci. Technol., **17** (3), 035010 (2008). DOI: 10.1088/0963-0252/17/3/035010
[34] T.M. Randolph, J.E. Polk. *An Overview of the Nuclear Electric Xenon Ion System (NEXIS) Activity*. 40th AIAA/ASME/SAE/ASEE Joint Propulsion Conf. and Exhibit, 2004-3450, 2004. DOI: 10.2514/6.2004-3450
[35] A.W. Hoskins, F.C. Wilson, M.J. Patterson, G.C. Soulas, J. Polaha, L. Talerico, J. Sovey. *Development of a Prototype Model Ion Thruster for the NEXT System*. 40th AIAA/ASME/SAE/ASEE Joint Propulsion Conf. and Exhibit, 2004-4111, 2004. DOI: 10.2514/6.2004-4111
[36] S. Mahalingam, Y. Choi, J. Loverich, P.H. Stoltz, B. Bias, J.A. Menart. *Fully Coupled Electric Field/PIC-MCC Simulation Results of the Plasma in the Discharge Chamber of an Ion Engine*. 47th AIAA/ASME/SAE/ASEE Joint Propulsion Conf. and Exhibit, 2011-6071, 2011. DOI: 10.2514/6.2011-6071
[37] H. Yoshida, H. Kawauchi, S. Takama, T. Maeda, T. Higuchi, K. Akai, Y. Hayakawa, K. Miyazaki, S. Kitamura, H. Nagano. *Performance Characteristics of a 35-cm Diameter Xenon Ion Thruster*. 32nd Joint Propulsion Conf. and Exhibit, 1996-2714, 1996. DOI: 10.2514/6.1996-2714
[38] Y. Hayakawa, H. Yoshida, S. Kitamura, K. Kajiwara, Y. Ohkawa. *Status of the 150-mN Ion Engine Research at JAXA*. 40th AIAA/ASME/SAE/ASEE Joint Propulsion Conf. and Exhibit, 2004-3969, 2004. DOI: 10.2514/6.2004-3969
[39] S. Kitamura, Y. Ohkawa, Y. Hayakawa, H. Yoshida, K. Miyazaki. *Overview and Research Status of the JAXA 150-mN Ion Engine*. 57th International Astronautical Congress, IAC-06-C4.4.1, 2006. DOI: 10.2514/6.iac-06-c4.4.01
[40] S. Kitamura, Y. Ohkawa, Y. Hayakawa, H. Yoshida, K. Miyazaki. Acta Astronautica, **61** (1–6), 360 (2007). DOI: 10.1016/j.actaastro.2007.01.010
[41] M.Y. Selivanov, A.S. Lovtsov. *IT-200PM Ring-Cusp Ion Thruster*. 36th International Electric Propulsion Conf., 2019-339, 2019
[42] M. Coletti, N. Wallace, S.B. Gabriel, D. Frollani, H. Simpson. *Ring Cusp Ion Engine Development in the UK*. 30th International Electric Propulsion Conf., 2015-130, 2015
[43] V.V. Koshlakov, K.V. Gotovtsev, L.E. Zakharenkov, A.V. Karevskiy, E.N. Kiryushin, A.S. Lovtsov, Yu.A. Oshev, A.V. Semenkin, A.E. Solodukhin, S.Yu. Fedotov, S.Yu. Fedyunin, A.G. Tsvetkov. Space Engineering Technol., **1** (36), 80 (2022). DOI: 10.33950/spacetech-2308-7625-2022-1-80-95

Translated by A.Akhtyamov